# On-chip Terahertz Spectroscopy of Liquid Mixtures

M. Swithenbank,* C. Russell,* A. D. Burnett,*† L. H. Li,*
E. H. Linfield,* A. G. Davies,* J. E. Cunningham,* and C. D. Wood.*
*School of Electronic and Electrical Engineering, University of Leeds, Leeds, LS2 9JT, UK.
†School of Chemistry, University of Leeds, Leeds, LS2 9JT, UK.
Email: el08m2s@leeds.ac.uk

***Abstract*—We demonstrate 'through-substrate' sensing of fluids for application in the terahertz spectroscopy of biological materials. This technique employs planar Goubau lines with integrated photoconductive material, formed on a flexible, thin polyimide substrate, and bonded to a microfluidic channel. Few-picosecond pulses are used to probe liquid samples confined within the channel, over a total interaction length of 4 mm, overcoming water-absorption limitations of free-space terahertz transmission measurements.**

## I. Introduction and Background

In recent years, free-space terahertz time-domain spectroscopy (THz-TDS) has become a well-established spectroscopic research tool. One particular application of increasing interest is the study of bio-molecular dynamics that occur on nanosecond to femtosecond timescales [1]. However, the strong absorption of THz signals in aqueous solutions imposes restrictions on the maximum sample thickness which may be measured, and limits correspondingly the interaction length between the sample and the probing THz radiation. On-chip THz devices, integrated with microfluidic systems, offer a potential solution [2]. Here, a THz pulse is generated at a substrate surface via laser excitation of embedded biased photoconductive switches (PCS). The pulse then couples into, and propagates along, a lithographically defined planar waveguide. The electric field associated with the THz pulse, which is confined to within 10's of microns of the substrate surface [3], can interact with the liquid under test (LUT) over long (mm) distances, whilst experiencing significantly reduced attenuation.

Microfluidic systems allow liquid manipulation on a sub-millimetre scale, thereby reducing the volume and cost of analytes [4]. At these length scales, interfacial forces, surface tension, and capillary forces dominate over gravitational forces, resulting in predictable laminar flows that allow spectroscopic information to be obtained, without turbulence and bubble formation interfering with measurements [5]. However, when integrated into on-chip THz devices, microfluidic channels can introduce time-domain reflection of a THz signal — from locations at which the channel crosses the transmission line — owing to abrupt changes in the local effective impedance. In this work, we introduce an alternative arrangement in which the fluidic channel is positioned on the other side of the substrate relative to the waveguide position. This removes restriction on the positioning of the microfluidic channel, which would otherwise be limited by the location of the PCS and electrical connections, and while also removing the interfacial reflections which can complicate subsequent analysis.

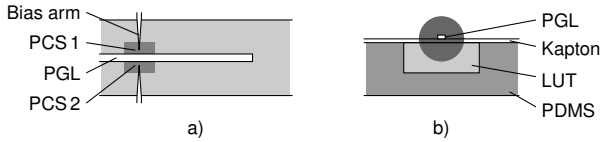


Fig. 1. (a) Schematic of a 2-mm-long reflection device showing the Ti:Au PGL aligned parallel to the microfluidic channel. The dark square shows the position of the LT-GaAs. (b) The cross-section of the device in (a), the dark circle represents the radial THz-field.

## II. Results

Here, reflection geometry PGL waveguides (as illustrated in Fig. 1) were fabricated by a procedure modified from that given in Ref. [6]. Briefly, 350-nm-thick low temperature (LT) GaAs was grown at 205 °C, using molecular beam epitaxy, on a 100-nm-thick AlAs layer, itself grown on a 500-μm-thick semi-insulating (SI) GaAs wafer. A layer of wax (Wax W, Apiezon) was deposited on the LT-GaAs, and the AlAs layer selectively etched in a HF:$H_2O$ solution (1:9). Supported by the wax, the released LT-GaAs layer was aligned on the polyimide (Kapton) substrate and left for five days to allow the formation of van der Waals bonds [7]. PCS were defined by etching 70 μm×70 μm squares into the LT-GaAs for 10 minutes in a dilute $H_2SO_4$:$H_2O_2$:$H_2O$ solution (1:8:950). A lithographically patterned layer of Ti:Au (10:150 nm) was deposited to define the PGL and bias arms.

Microfluidic channels were constructed from polydimethylsiloxane (PDMS) (Sylgard 184, Dow Corning) mixed in a 1:10 (curing agent to base) ratio, and poured over a mould formed from SU-8 50 photoresist, designed to produce a channel depth of 400 μm — this depth selected to be greater than the maximum extent (∼100 μm) of the evanescent field about the PGL [8] to ensure saturation. The cast PDMS was bonded to the underside of the Kapton substrate by forming a chemical bond between the two materials [9]. The surfaces to be bonded were exposed to an $O_2$-plasma (50 W, 1 minute), forming hydroxyl groups. A 2 % (v/v) aqueous solution of 3-aminopropyltriethoxysilane was poured over the polyimide film, and a 2 % (v/v) solution of 3-glycidoxypropyltriethoxysilane in isopropanol (IPA) was poured over the PDMS channel. Each solution was left for

20 minutes, after which the amine and epoxy-fuctionalised surfaces were washed in deionised (DI) $H_2O$ and dried with $N_2$. The surfaces were brought into contact, such that the channel was aligned with the PGL sensing region, and bonded at room temperature for one hour. A strong amine–epoxy bond was formed, which has been shown to withstand channel pressures of 5 bar [9]. Inlet and outlet ports were formed using silicone tubing. The inlet was connected to a syringe pump to provide control over the flow rate of the LUT.

THz signals were generated when optical pulses from a Ti:sapphire laser (100 fs duration, 800 nm centre wavelength, 80 MHz repetition rate, and 10 mW average power) were focused onto PCS 1 (see Fig. 1a), to which a 20 V DC bias was applied. The pulses propagated along the PGL and were detected at PCS 2, which was illuminated by an optically delayed, mechanically chopped laser beam, allowing the resultant picosecond pulse to be measured using lock-in detection. The time-domain response was recorded by measuring the transient photocurrent of this PCS as the arrival time of the excitation pulse was varied with respect to the probing pulse.

The extent of evanescent field about the PGL used here is approximately 100 µm [8]. It is therefore necessary for the substrate thickness to be less than this value in order to perform THz-TDS of sample liquids in a channel bonded beneath the substrate. This criteria was satisfied by fabricating the device on a 50-µm-thick Kapton film as per Fig. 1. Pulses which are excited at PCS 1 propagate along the PGL, and are reflected off the open-circuit stub before detection at PCS 2. As the generated and reflected THz signals are both measured in a single time-domain response (Fig. 2a), it is critical that there is sufficient time delay — controlled by the length of the sensing region — to allow isolation of each feature for analysis. Yet, longer propagation distances increase waveguide losses, and so a 2-mm-long sensing region was chosen for these measurements. For analysis, the transition between the input and output pulses was chosen to be 14 ps, as illustrated in Fig. 2a.

The channel was filled with mixtures of IPA and DI-$H_2O$ in which the volume fraction of IPA was increased from 0–100 % in 10 % increments. The measured responses are shown in Fig. 2a and b. The time-domain responses comprised two main features: an 'input' pulse centred at 0 ps, and a time-delayed pulse reflected from the open circuit stub with a total round trip of 4 mm. The frequency responses shown in Fig. 2b, with a resolution of 7 GHz, were found by performing a Fourier transform on the input and output pulses from the data in Fig. 2a. The bandwidth of the generated input pulse was approximately 1.2 THz, and the strong attenuation by the LUTs limited the output bandwidth to less than 350 GHz. The broadening of the input pulse as the IPA fraction was increased is thought to be a result of heating effects owing to the thermal conductivities of the LUTs (0.15 and 0.6 $\mathrm{W\,m^{-1}\,K^{-1}}$ for IPA and DI-$H_2O$ respectively [10]). Despite this, the change in frequency response was less than the standard deviation of repeated measurements, and therefore negligible.

The results given in Fig. 2a can be used to approximate the

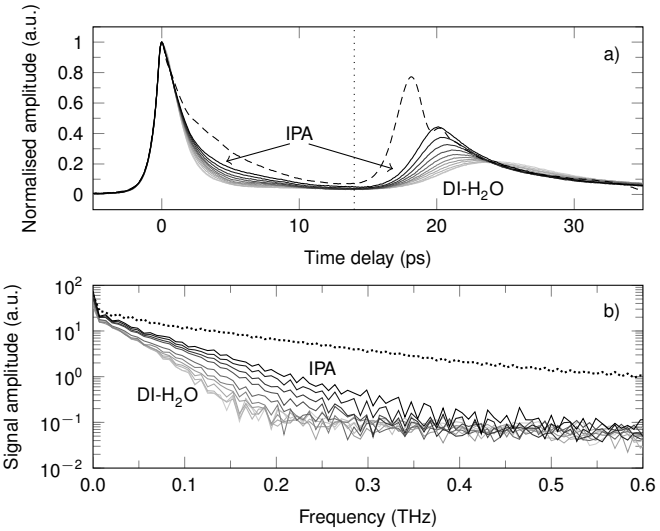


Fig. 2. (a) Normalised TDS response of a 2-mm-long reflection PGL when the channel was empty (dashed), and filled with mixtures of IPA and DI-$H_2O$ (greyscale). The dotted line indicates the input pulse cut-off. (b) The Fourier transform of an input pulse (dotted), and the reflected data (black).

permittivity contribution of the LUT across the measured frequency band. The effective permittivity, $\varepsilon_{\mathrm{eff}}$ of the transmission line was calculated using the time delay of the reflected pulse $t_{\mathrm{g}}$ for a given propagation length $l$, such that

$$\varepsilon_{\mathrm{eff}} = \left(\frac{ct_{\mathrm{g}}}{l}\right)^2, \tag{1}$$

where $c$ is the speed of light.

Assuming a circular THz field of radius $r$, with area $A_{\mathrm{THz}}$, the areas of intersection between the components of the three-layer system illustrated in Fig. 1b and the THz field can be used to calculate the permittivity contribution of the LUT, $\varepsilon_{\mathrm{sam}}$, as follows [8]:

$$\varepsilon_{\mathrm{sam}} = \frac{\varepsilon_{\mathrm{eff}}A_{\mathrm{THz}} - \varepsilon_{\mathrm{sup}}A_{\mathrm{sup}} - \varepsilon_{\mathrm{sub}}A_{\mathrm{sub}}}{A_{\mathrm{sam}}}, \tag{2}$$

where $A_{\mathrm{sup}}$, $A_{\mathrm{sub}}$, and $A_{\mathrm{sam}}$ are the areas of intersection between the evanescent THz field and the superstrate $\varepsilon_{\mathrm{sup}}$, substrate $\varepsilon_{\mathrm{sub}}$, and LUT respectively. For a substrate of thickness $d$, the areas of intersection can be defined as

$$A_{\mathrm{sup}} = \frac{\pi r^2}{2}, \tag{3}$$

$$A_{\mathrm{sub}} = \theta r^2 + rd\sin\left(\frac{\pi}{2} - \theta\right), \tag{4}$$

and

$$A_{\mathrm{sam}} = \frac{\pi - 2\theta}{2}r^2 - rd\sin\left(\frac{\pi}{2} - \theta\right), \tag{5}$$

where

$$\theta = \frac{\pi}{2} - \cos^{-1}\left(\frac{d}{r}\right). \tag{6}$$

For example, the time-of-flight of pulses when the channel was filled with IPA was 19.6 ps which, according to Eq. (1), equates to an $\varepsilon_{\mathrm{eff}}$ of 2.16. Given an air superstrate and Kapton substrate, $\varepsilon_{\mathrm{sup}}$ and $\varepsilon_{\mathrm{sub}}$ were equal to 1 and 3.6 [11]

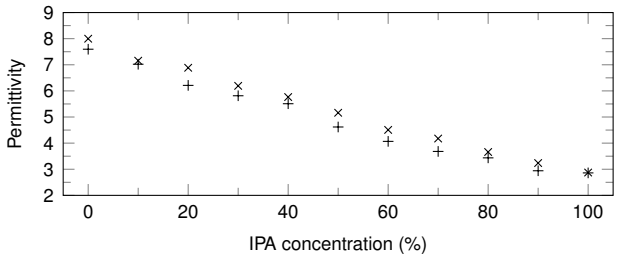


Fig. 3. The calculated permittivity contribution of IPA:DI-$H_2O$ solutions measured with a microfluidic PGL device ($\times$) and a freespace THz-TDS system at 100 GHz ($+$). Note that the data points overlap at an IPA concentration of 100 %.

respectively. The permittivity of IPA in this frequency band was therefore calculated to be 2.87, which is in agreement with data published in this range [12]. These calculations were repeated across the range of IPA:DI-$H_2O$ mixtures, and the results are shown in Fig. 3.

Data collected from the microfluidic PGL device were verified by measuring the same solutions in a freespace THz-TDS system with a bandwidth of 0.1 to 2.5 THz, similar to that described in Ref. [13]. The LUTs were held in a variable pathlength flowcell fitted with two 2-mm-thick quartz windows separated by a 100-µm-thick PTFE spacer. The LUTs were measured, and their frequency-dependent permittivity calculated at 100 GHz (the center of the PGL device's usable bandwidth), using the method described in Ref. [13].

As shown in Fig. 3, the results from the two systems are in agreement, yet the permittivities calculated from the PGL device are consistently greater than those from the freespace system, suggesting a systematic error as a result of the model used. This is consistent with previous work showing the asymmetric THz field distribution found in PGL devices where the substrate permittivity is greater than the superstrate [14]. Therefore, the area of interaction between the LUT and the THz field is greater than that given by Eq. (5), resulting in an overestimate of $\varepsilon_{\text{sam}}$ by Eq. (2). To reduce the effects of this discrepancy for high-permittivity samples, a more accurate model of the field distribution about the PGL transmission line is required. However, analytically solving PGL systems is a non-trivial task owing to the lack of identifiable boundary conditions which are required to determine the electric and magnetic fields in other transmission line geometries, such as coplanar or microstrip [15].

## III. Conclusion

A technique for the measurement of microfluidic systems, using on-chip terahertz time-domain spectroscopy with planar Goubau lines was reported. It has been demonstrated that PGL devices with overlaid microfluidic channels can support an evanescent field with frequency components in the THz range across a 4-mm-long interaction-length. The reflection geometry adopted here allowed both the input and output pulses to be recorded in a single measurement. Time-of-flight measurements allowed the permittivity contribution of the LUT to be calculated from a model of the microfluidic device structure. In further work, the output bandwidth of these devices can be improved by reducing the interaction length, hence reducing the absorption and dispersion of propagating fields. However, it will be necessary to use a transmission geometry in which the input and output pulses are measured independently, given the requirement for them to be temporally distinct.

Results were verified by measurements from a flowcell placed in a freespace THz-TDS system. We found that LUT permittivities calculated from microfluidic PGL data were greater than those measured in a freespace system. We attribute this discrepancy to the asymmetric field distribution arising from a substrate permittivity greater than that of the superstrate. Future development of this technique will require a more comprehensive PGL model that accounts for field distribution to improve accuracy for high-permittivity samples.

## Acknowledgment

This work was supported by funding from the EPSRC (UK), the ERC programme 'TOSCA', the DTRA (US) (HDTRA1-14-C-0013), the Royal Society, and the Wolfson Foundation.

## References

[1] K. A. Niessen, M. Xu, and A. G. Markelz, "Terahertz optical measurements of correlated motions with possible allosteric function", Biophys. Rev. 7, 2, 201–216, 2015.

[2] T. Ohkubo, M. Onuma, J. Kitagawa, and Y. Kadoya, "Micro-strip-line-based sensing chips for characterization of polar liquids in terahertz regime", Appl. Phys. Lett. 88, 212511, 2006.

[3] D. Gacemi, A. Degiron, M. Baillergeau, and J. Mangeney, "Identification of several propagation regimes for terahertz surface waves guided by planar Goubau lines", Appl. Phys. Lett. 103, 191117, 2013.

[4] E. K. Sackmann, A. L. Fulton, and D. J. Beebe, "The present and future role of microfluidics in biomedical research", Nature 507, 7491, 181–189, 2014.

[5] H. Song, D. L. Chen, and R. F. Ismagilov, "Reactions in droplets in microfluidic channels", Angew. Chem. Int. Edit. 45, 44, 7336–7356, 2006.

[6] J. Cunningham, C. Wood, A. G. Davies, I. Hunter, E. H. Linfield, and H. E. Beere, "Terahertz frequency range band-stop filters", Appl. Phys. Lett. 86, 21, 213503, 2005.

[7] E. Yablonovitch, D. M. Hwang, T. J. Gmitter, L. T. Florez, and J. P. Harbison, "Van der Waals bonding of GaAs epitaxial liftoff films onto arbitrary substrates", Appl. Phys. Lett. 56, 24, 2419–2421, 1990.

[8] C. Russell, C. D. Wood, A. D. Burnett, L. Li, E. H. Linfield, A. G. Davies, and J. E. Cunningham, "Spectroscopy of polycrystalline materials using thinned-substrate planar Goubau line at cryogenic temperatures", Lab Chip 13, 4065–4070, 2013.

[9] L. Tang, and N. Y. Lee, "A facile route for irreversible bonding of plastic-PDMS hybrid microdevices at room temperature", Lab Chip 10, 1274–1280, 2010.

[10] M. J. Assael, E. Charitidou, and W. A. Wakeham, "Absolute measurements of the thermal conductivity of mixtures of alcohols with water", Int. J. Thermophys. 10, 4, 793–803, 1989.

[11] P. D. Cunningham, N. N. Valdes, F. A. Vallejo, L. M. Hayden, B. Polishak, X.-H. Zhou, J. Luo, A. K.-Y. Jen, J. C. Williams, and R. J. Twieg, "Broadband terahertz characterization of the refractive index and absorption of some important polymeric and organic electro-optic materials" J. Appl. Phys. 109, 043505, 2011.

[12] T. Sato, and R. Buchner, "Dielectric relaxation spectroscopy of 2-propanol–water mixtures", J. Chem. Phys. 118, 10, 4606–4613, 2003.

[13] M. Naftaly, and R. E. Miles, "Terahertz time-domain spectroscopy: A new tool for the study of glasses in the far infrared", J. Non-Cryst. Solids 351, 3341–3346, 2005.

[14] A. Treizebré, B. Bocquet, Y. Xu, and R. G. Bosisio, "New THz excitation of planar Goubau line", Microw. Opt. Techn. Let. 50, 11, 2998–3001.

[15] H. E. Green, "The numerical solution of some important transmission-line problems", IEEE MTT-13, 5, 676–692, 1965.